J Physiol 588.13 (2010) pp 2373–2390

The Journal of Physiology

Mechanisms of synchronous activity in cerebellar Purkinje cells

Andrew K. Wise[1], Nadia L. Cerminara[1], Dilwyn E. Marple-Horvat[1,2] and Richard Apps[1]

[1] *Department of Physiology and Pharmacology, University of Bristol, UK*
[2] *Institute for Biomedical Research into Human Movement and Health (IRM), Manchester Metropolitan University, UK*

Complex spike synchrony is thought to be a key feature of how inferior olive climbing fibre afferents make their vital contribution to cerebellar function. However, little is known about whether the other major cerebellar input, the mossy fibres (which generate simple spikes within Purkinje cells, PCs), exhibit a similar synchrony in impulse timing. We have used a multi-microelectrode system to record simultaneously from two or more PCs in the posterior lobe of the ketamine/xylazine-anaesthetized rat to examine the relationship between complex spike and simple spike synchrony in PC pairs located mainly in the A2 and C1 zones in crus II and the paramedian lobule. PC pairs displaying correlations in the occurrence of their complex spikes (coupled PCs) were usually located in the same zone and were also more likely to exhibit correlations in the timing of their spontaneous simple spikes and associated pauses in activity. In coupled PCs, synchrony in both complex spike and simple spike activity was enhanced and the relative timing in the occurrence of complex spikes could be altered by peripheral stimulation. We conclude that the functional coupling between PC pairs in their complex spike and simple spike activity can be significantly modified by sensory inputs, and that mechanisms besides electrotonic coupling are involved in generating PC synchrony. Synchronous activity in multiple PCs converging onto the same cerebellar nuclear cells is likely to have a significant impact on cerebellar output that could form important timing signals to orchestrate coordinated movements.

(Resubmitted 9 March 2010; accepted after revision 4 May 2010; first published online 4 May 2010)
Corresponding author A. K. Wise: Bionic Ear Institute, 384-388 Albert St, East Melbourne, Vic, Australia, 3002. Email: awise@bionicear.org

Abbreviations CS, complex spike; CV, coefficient of variation; PC, Purkinje cell; PSTH, peri-stimulus time histogram; SI, synchrony index; SS, simple spike; T0, time zero.

Introduction

The cerebellar cortex is divided into numerous rostro-caudally oriented zones each defined by its climbing fibre input from a discrete territory within the inferior olive. In turn, the Purkinje cells (PCs) located within each zone provide a correspondingly highly organized and convergent cortico-nuclear projection to the cerebellar and vestibular nuclei (for review see e.g. Voogd & Glickstein, 1998). The functional significance of these relationships remains ill-defined but the existence of cortical zones strongly supports the view that investigations of cerebellar function should be framed in terms of their organization (Apps & Garwicz, 2005; Apps & Hawkes, 2009). The importance of climbing fibres is further emphasized by the fact that they generate a powerful depolarizing event, termed a complex spike, in their target PCs (Eccles *et al.* 1966). By contrast, the other major source of input to the cerebellar cortex, the mossy fibres, originate from numerous CNS sources and act indirectly on PCs via the granule cell–parallel fibre system, generating conventional action potentials known as simple spikes (Thach, 1967). PCs are also known to generate intrinsic simple spike activity in the absence of synaptic inputs (Woodward *et al.* 1974; Llinás & Sugimori, 1980; Hounsgaard & Midtgaard, 1988; Häusser & Clark, 1997; Cerminara & Rawson, 2004).

Typically, individual PCs discharge complex spikes at low rates (1–2 Hz, Thach, 1968; Armstrong & Rawson, 1979), but they usually discharge simple spikes at rates of between 10 and 100 Hz during motor performance (e.g. Armstrong & Rawson, 1979; Cerminara *et al.* 2009). Because simple spike frequency modulation appears to dominate PC output during behaviour, simple spikes are thought to be important for the moment-to-moment operation of the cerebellum. Yet small groups of PCs,

DOI: 10.1113/jphysiol.2010.189704

located in rostrocaudally aligned strips in the cerebellar cortex (presumably corresponding to parts of individual zones), can fire complex spikes in tight synchrony (Bell & Kawasaki, 1972; Llinás & Sasaki, 1989; Sasaki *et al.* 1989; Sugihara *et al.* 1995; Welsh *et al.* 1995; Wylie *et al.* 1995; Lang *et al.* 1996, 1999; Lang, 2002, 2003; Ozden *et al.* 2009). As a consequence, it has been suggested that synchronous complex spike activity in ensembles of PCs influences cortico-nuclear output sufficiently to act as a precise timing signal related to coordination of on-going movements (Llinás & Sasaki, 1989; Welsh & Llinás, 1997).

It is also possible that PCs located in the same cortical zone could display temporal correlations in their simple spikes. Since simple spikes probably constitute more than 90% of PC activity, such an arrangement is likely to have a significant impact on cortico-nuclear output, and thus have a profound influence on cerebellar contributions to movement control. However, to date, few studies (Bell & Grimm, 1969; Bell & Kawasaki, 1972; De Zeeuw *et al.* 1997; Schwarz & Welsh, 2001) have analysed both complex spike and simple spike firing patterns in simultaneous recordings from individual PCs, and the effects of peripheral afferent drive on complex spike and simple spike temporal relations are not well characterized.

In the present study we provide evidence that PC pairs located within the same cortical zone (the vermal A2 and paravermal C1 zones) can display correlations in the timing of both their complex spike and simple spike activity. For the latter, both the timing of spikes and pauses in activity were found to be correlated. Furthermore, the functional coupling of both simple spikes and complex spikes can be enhanced, and the timing relationship of complex spikes significantly altered by peripheral afferent drive, which therefore represents a powerful mechanism by which both major types of cerebellar input could influence cortico-nuclear output during movement.

Methods

Ethical approval

Adult Wistar rats ($n = 15$) with an average weight of 300 g were used in the present study. Experiments were performed in accordance with the UK Animals (Scientific Procedures) Act 1986. All experimental procedures were approved by the University of Bristol institutional animal licence advisory group and complied with published regulations on animal experimentation (Drummond, 2009). Animals were anaesthetized with ketamine (100 mg kg^{-1}) and xylazine (5 mg kg^{-1} I.P.). The depth of anaesthesia was regularly assessed by a paw pinch to monitor reflex muscle tone, and supplementary doses of anaesthetic were administered as required. At the conclusion of the experiment the animal was killed with an anaesthetic overdose. Local anaesthetic (5% Xylocaine ointment, AstraZeneca, UK) was applied to the external auditory meatus to minimize sensory afferent activity. The rat was then placed in a stereotaxic frame. A heated blanket regulated by feedback from a rectal thermometer maintained core body temperature at 37°C.

Electrophysiological stimulation and recording

A small craniotomy exposed the left dorsal surface of the posterior lobe of the cerebellum. The dura was removed allowing access to the medial parts of crus II, the paramedian lobule and copula pyramidis. Bipolar percutaneous stimulating electrodes were inserted into the contralateral whisker pad and the ipsilateral forelimb. Cortical zones in the medial aspect of crus II, paramedian lobule and copula pyramidis were mapped electrophysiologically by recording the mediolateral sequence of climbing fibre field potentials evoked by ipsilateral forelimb or contralateral face stimulation, as described previously (Atkins & Apps, 1997; Pardoe & Apps, 2002). In brief, percutaneous electrical stimulation (single pulse; 0.1 ms duration) at 1 s intervals applied to the ipsilateral distal forelimb ('forelimb') or contralateral whisker pad ('face'), at an intensity sufficient to evoke a small but visible muscle twitch from the stimulated region, was used to set up volleys in ascending spino-cerebellar paths. Evoked climbing fibre field potentials were recorded extracellularly from the cerebellar surface using tungsten-in-glass microelectrodes (tip diameter ~50 μm). Individual cortical zones were defined in terms of the peripheral stimulation site that evoked the largest climbing fibre field potentials within that zone: the A2 and C1 zones were defined by responses evoked by contralateral face and by short latency responses evoked by ipsilateral forelimb stimulation, respectively (cf. Atkins & Apps, 1997). The evoked fields were recorded differentially, amplified and bandpass filtered (30 Hz to 5 kHz), and a Humbug device (Quest Scientific, North Vancouver, British Columbia, Canada) was used to eliminate any 50 Hz electrical interference. Field potentials evoked from each recording site were digitized on-line (sampling rate 2.5 kHz) using a Cambridge Electronic Design (CED, Cambridge, UK) 1401 analog-to-digital converter and Spike2 software (CED).

The zonal electrophysiology was used to guide the insertion of four independently controlled glass-insulated tungsten microelectrodes (Alpha-Omega, Israel) that enabled simultaneous recordings from up to four individual PCs. The microelectrode array had a square design with an approximate spacing of 500 μm between recording electrodes (700 μm diagonally). Single unit recordings were bandpass filtered (300 Hz to 5 kHz), digitized (21 kHz) and stored on the computer hard disk. Only recordings of PC pairs with sufficient signal-to-noise to reliably discriminate between complex spikes and

simple spikes were used in the present analysis. Single unit PCs were identified by the presence of complex spikes, while the characteristic cessation in simple spike activity following each complex spike (duration *ca* 10 ms) was used to confirm that both types of activity were derived from the same cell. Simple spike and complex spike activity were discriminated independently via a template-matching algorithm (principal component analysis, Spike2, CED). In most cases simple spikes and complex spikes were reliably identified by differences in waveform of the initial component of the spikes. However, on occasions where the initial component of the complex spike and the simple spike were similar, individual complex spikes were identified by the occurrence of their secondary components. The spontaneous and evoked activity of complex spikes and simple spikes of individual PCs were obtained in the same recording session. Typically ∼700 complex spikes and ∼8000 simple spikes were recorded from each PC for off-line analysis.

Classification of PC zonal origin

A number of criteria were used to help classify individual PCs as located within a particular cerebellar cortical zone. First, the site where each microelectrode penetration was made perpendicular to the cortical surface was carefully noted in relation to major anatomical landmarks. In particular, previous studies have shown that in the paramedian lobule the A2 zone is located immediately lateral to the paravermal vein where it extends laterally for about 0.6 mm (Atkins & Apps, 1997). Second, the distribution of field potentials evoked on the cerebellar surface by peripheral stimulation was used to aid location of the single unit recording tracks in relation to the electrophysiologically defined boundary between the A2 and C1 zones (Atkins & Apps, 1997; Pardoe & Apps, 2002). And third, every PC was tested for its complex spike response to peripheral stimulation (for further details see below). If the recording track was (i) located no more than 0.6 mm lateral from the paravermal vein, (ii) less than 2.5 mm from the cortical surface, and (iii) the cell responded to contralateral face stimulation with a robust increase in complex spikes with a short onset latency (usually <30 ms), then it was classified as located in the A2 zone. Similarly, if the recording track was (i) between 0.6 and 1.3 mm lateral from the paravermal vein, (ii) less than 2.5 mm from the cortical surface, and (iii) the cell responded to ipsilateral forelimb stimulation with a robust increase in complex spikes with a short latency (usually <25 ms), then it was classified as located in the C1 zone. One PC was tentatively classified as located within the C2 zone because of its lateral location, and because it displayed longer latency (∼35 ms) robust complex spike responses to both forelimb and face stimulation.

Data analysis

Peri-stimulus time histograms (PSTHs) were generated separately for complex spike (5 ms bins, 100 bins) and simple spike (1 ms bins, 100 bins) responses to stimulation of the face and forelimb. Each PSTH was usually based on >700 stimulus trials over a recording period of ∼25 min. Similarity between PSTHs constructed for complex spike and simple spike activity within a PC pair was assessed by comparing the spike counts in each time bin.

Correlations in spontaneous activity

The strength of synchrony of complex spikes and simple spikes between PC pairs was determined by constructing cross-correlograms. Since complex spikes are ∼10 ms and simple spikes ∼1 ms in duration (see Results), cross-correlograms of the spike trains were therefore constructed with 10 ms and 1 ms time bins, respectively. For spontaneous complex spike activity, pairs of PCs were categorized as 'coupled PCs' if there was a statistically significant peak (exceeding 99% confidence limits) for one or both 10 ms time bins either side of time zero in the cross-correlogram (the two 10 ms bins either side of zero are referred to as 'time zero' in Results). Pairs of cells were classified as 'non-coupled PCs' if both these time bins did not exceed 99% confidence limits. A bin width of 10 ms to define complex spike synchrony is compatible with some previous studies (Lou & Bloedel, 1992; Wylie *et al.* 1995) but is less stringent than others (e.g. Llinás & Sasaki, 1989; Welsh *et al.* 1995; Lang *et al.* 1999). To quantify the correlation in spontaneous complex spike activity the standard cross-correlation coefficient was used as a synchrony index (SI) $SI = SS_{xy}/\sqrt{SS_{xx}SS_{yy}}$ where SS = sum of square (see Llinás & Sasaki, 1989; Wylie *et al.* 1995). The synchrony index takes into account any difference in firing rate between the two cells.

Cross-correlograms for spontaneous simple spike activity were also constructed for coupled and non-coupled PC pairs using 1 ms time bins and smoothed over three bins. The statistical significance of any peak in the cross-correlogram at time zero (the two 1 ms bins either side of zero) was determined by comparing the peak value (average of the two 1 ms bins either side of zero) to the mean value in the time period ranging from between −2 and −1 s before time zero (termed baseline in Fig. 2*B*). The average value of this one second baseline time period provided an estimate of the probability and its S.D. of the PC pair firing simple spikes by chance in any particular time bin. A peak at time zero was considered to be statistically significant if it was larger than the baseline average by 1.96 × S.D. (i.e. $P < 0.05$). To permit comparisons between PC pairs, the time zero peak was expressed as a percentage increase in the simple spike firing probability with respect to baseline. For example, a PC pair

may have a baseline probability in the correlogram of 0.002 (during the −2 to −1 s time period). If the probability at time zero was measured at 0.004 then this would represent a 100% increase.

Correlations during peripheral stimulation

To determine whether complex spike synchrony in coupled PCs could be modified by peripheral input, cross-correlograms (10 ms bins) were constructed using spikes occurring in the 0–500 ms response time window after face and forelimb stimulation. As in previous studies (e.g. Schwarz & Welsh, 2001) an adjustment to the cross-correlogram was necessary to exclude correlations resulting from any independent but stimulus-locked response of each cell. Such stimulus-locked correlations can be removed by subtracting the 'shuffle predictor' from the raw cross-correlogram (Gerstein & Perkel, 1972). The shuffle predictor is a cross-correlation that is generated by rearranging (shuffling) the trial order for each PC separately. For instance, the spike train generated by PC1 in the *n*th trial is compared to the spike train from PC2 from the *n*th ± *x*th trial. The shuffling of the two spike trains removes any intrinsic correlation that may be present within the same trials so any correlation that remains represents activity due to the two cells responding at similar times to the stimulus. The subtraction of this predictor from the raw cross-correlogram produces a 'shuffle-corrected cross-correlogram'. A shuffle predictor using 10,000 shuffle combinations was used to remove any independent but stimulus-locked correlations.

To quantify any observed changes in complex spike synchrony during peripheral stimulation, the amplitude of the time zero peak of the shuffle-corrected cross-correlograms was measured for face and forelimb stimulation and compared with the cross-correlation for spontaneous complex spike activity (see Fig. 4). The data were further separated into two shorter time periods (0–100 ms and 100–500 ms post stimulus, see Fig. 4*A*) to determine whether any changes in complex spike synchrony occur shortly after the stimulus or within a longer time frame. Average firing probability was calculated for complex spike activity of coupled and non-coupled PCs during spontaneous activity and when driven by peripheral stimulation.

Shuffle-corrected correlograms (1 ms bin smoothed over 3 bins) were also constructed to analyse simple spike activity in the initial 0–100 ms time window following peripheral stimulation (see Fig. 6). Any time zero peak that exceeded the 99% confidence limits was considered to be statistically significant. The size of each time zero peak was measured for each PC pair and the average firing probability for coupled and non-coupled PCs was calculated for their spontaneous simple spike activity and compared to simple spike activity evoked in response to forelimb and face stimulation.

To determine whether there was any change in the temporal relationship (time shift) of complex spike or simple spike synchrony during peripheral stimulation, the time of the peak in the shuffle-corrected cross-correlograms was compared to the time of the corresponding peak observed in the cross-correlogram constructed for spontaneous activity. To obtain a more accurate indication of the timing of the peak, shuffle-corrected cross-correlograms were constructed with 1–2 ms bins (smoothed over 3 bins), for complex spikes or simple spikes that occurred in the 0–100 ms time window after the stimulus.

Correlations in simple spike pauses

In addition to the well-known complex spike-induced cessation in simple spike activity, simple spikes can also display longer periods of inactivity ('pauses'). Additional analysis was therefore carried out to determine whether coupled PCs had a tendency to display temporally correlated pauses in their simple spikes. A pause was defined as any period of simple spike inactivity that was in the top 5% of interspike intervals for that PC (e.g. if 95% of the simple spike intervals for a cell were less than 100 ms then any interval longer than 100 ms was considered a pause).

For each pause in a train of simple spikes, the spike at the start and end of each period of inactivity was identified (pause on and pause off, respectively) and these time points were used to construct three different cross-correlograms between PC pairs (5 ms bins averaged over 3 bins): (i) pause on *versus* on, to examine the timing between the onset of a pause in each cell; (ii) pause off *versus* off, to examine the timing of cessation of pauses in each cell; and (iii) pause on *versus* off, to examine the relationship between onset of a pause in one cell and cessation of a pause in the other cell. For each cross-correlogram the average of the ±5 ms bin (the time zero value) was calculated and compared to the baseline probability of a random relationship in simple spike pause timing (average of the probability during −2 to −1 s time bins).

Statistics

Data are presented as mean ± S.E.M. (or S.D. when indicated). For each spike train (complex spikes and simple spikes considered separately) a coefficient of variation (CV) was calculated as an indicator of temporal variability using the equation: CV = (S.D./mean)/100. To compare the pattern of modulation by peripheral stimulation in pairs of simultaneously recorded PCs

their PSTHs were analysed using the Pearson correlation. Parametric data were analysed using either Student's paired or unpaired *t* test or repeated measures ANOVA with Student–Newman–Keuls *post hoc* test, and two-way repeated ANOVA (with category, i.e. coupled and non-coupled PCs and simple spike pause as main factors) followed by Holm-Sidak *post hoc* comparison. For non-parametric data, the statistical analysis used was either the Mann–Whitney test or Friedman repeated measures ANOVA with the Dunn *post hoc* test as appropriate. Non-normal distributions were tested with the Kolmogorov–Smirnov test.

Results

In the present study, the overwhelming majority of recording sites were located in the medial aspect of crus II and the paramedian lobule (within ∼1.3 mm of the lateral edge of the paravermal vein, see Fig. 1*C* and *D*). Sufficient numbers of complex spikes and simple spikes for correlation analysis were reliably discriminated from one another in the spike trains obtained from a total of 45 PCs. Of these, 18 were identified as located in the A2 zone, 8 in the C1 zone and 1 in the C2 zone. The remainder ($n = 18$) could not be reliably classified (see Methods for details of classification). An example of single unit recordings obtained from one pair of PCs located in the A2 zone is shown in Fig. 1*B*.

During a recording period of spontaneous activity (average sample time of 26 min) complex spikes occurred with a frequency of 0.53 ± 0.33 Hz (mean ± S.D.; range 0.1–1.6 Hz), and had an average CV of 0.93 ± 0.24 (S.D.). The duration of complex spikes (time from onset of initial spike to start of last spikelet) was measured from periods of spontaneous and evoked activity for a total of 31 PCs. On average, complex spike duration was 9.8 ± 3.3 ms (S.D.) (based on a sample of 64,827 complex spikes). There was no significant difference in the duration of spontaneous complex spikes as compared to those evoked by peripheral stimulation (paired *t* test, $n = 31$, $P = 0.5$). Auto-correlations showed that a small proportion of the PCs (6/45, 13%) exhibited oscillations in their spontaneous complex spike activity, in which three or more complex spikes occurred at regular interspike intervals (oscillation frequency range 6–12.5 Hz).

The spontaneous firing rate of the simple spikes of the same PCs was on average 30.4 ± 13.5 Hz (S.D.) (range 1.8–57.6 Hz), and their CV was 2.64 ± 3.83 (S.D.). Like complex spike activity, oscillations in the spike trains of spontaneous simple spikes were present in only a small proportion of the same PCs (7/45, 15.5%, oscillation frequency range 34–55 Hz). Since no relationship was evident between the presence (or absence) of oscillations in

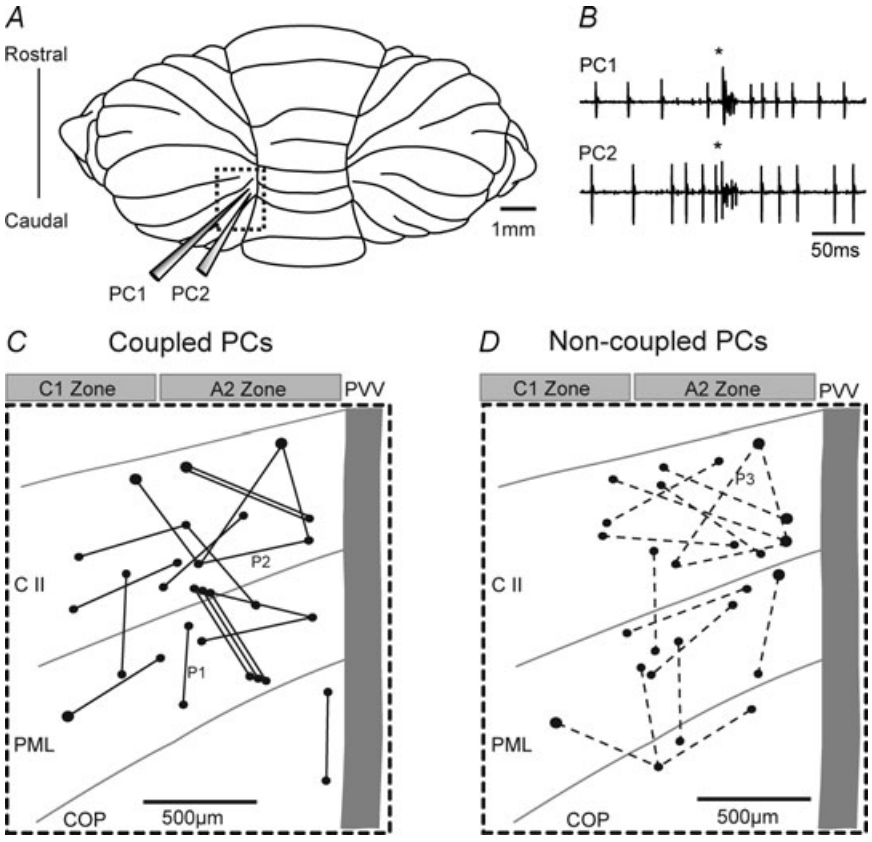

Figure 1. Location of coupled and non-coupled PC pairs
A, schematic diagram of the paramedian lobule of the rat cerebellum (dashed box). An array of four microelectrodes in a square configuration (only 2 shown) was used to record extracellular single unit activity. The spacing between the electrodes was 500 or 700 μm. *B*, example traces of two simultaneously recorded PCs (a coupled PC pair) generating spontaneous simple spikes and synchronous complex spikes (*). *C* and *D*, schematic representation of the cortical location of coupled PC pairs (*C*; continuous lines, $n = 19$) and non-coupled PC pairs (*D*; dashed lines, $n = 16$). PCs were predominantly located in the C1 and A2 zones in the medial crus II (C II), the paramedian lobule (PML) and the copular pyramidis (COP). All PC pairs were located within 1.3 mm from the lateral edge of the paravermal vein (PVV). The PSTHs for three PC pairs (P1, P2 and P3) are described in Fig. 3.

complex spike or simple spike activity and any synchrony between PC pairs, this phenomenon was not studied further.

Synchrony in spontaneous complex spike and simple spike activity

A total of 35 PC pairs were recorded simultaneously. Eight were classified as A2–A2 pairs; one was a C1–C1 pair; four were A2–C1 pairs, and the remainder had at least one cell of the pair that could not be reliably classified. A total of 19/35 (54%) of the PC pairs displayed statistically significant cross-correlations in the timing of their spontaneous complex spikes (termed coupled PCs). Complex spike synchrony index values ranged from 0.024 to 0.37 (mean ± S.E.M.; 0.09 ± 0.02, see for example Fig. 2*A*). The highest synchrony index scores were obtained for coupled PCs located within the same (A2) zone. The average synchrony index of PC pairs located within the same zone (A2 or C1) was about 70% larger than the average synchrony index for PC pairs located in different zones (0.12 ± 0.04, $n = 9$ and 0.07 ± 0.01, $n = 4$, respectively); however, this difference did not reach statistical significance (unpaired t test, Welch corrected, $P = 0.2$). In the remaining 16 PC pairs no statistically significant temporal relationship in the occurrence of spontaneous complex spikes was observed (termed non-coupled PCs).

In two of the coupled PCs no simple spike activity was recorded, therefore a total of 17 coupled PCs were available for analysis of simple spike cross-correlations. Of these, 11/17 (65%) also displayed a statistically significant peak in simple spike activity, based on the analysis of their cross-correlograms constructed with 1 ms bin width (see for example Fig. 2*B*). Overall, the peak in the simple spike cross-correlations for all 17 coupled PCs represented, relative to baseline probabilities of discharge, an average increase in synchronous firing of 7.5 ± 1.96%. Additional analysis was carried out on simple spike cross-correlations using wider bins (10 ms and 20 ms bin widths) in order to evaluate correlations in simple spike activity over longer

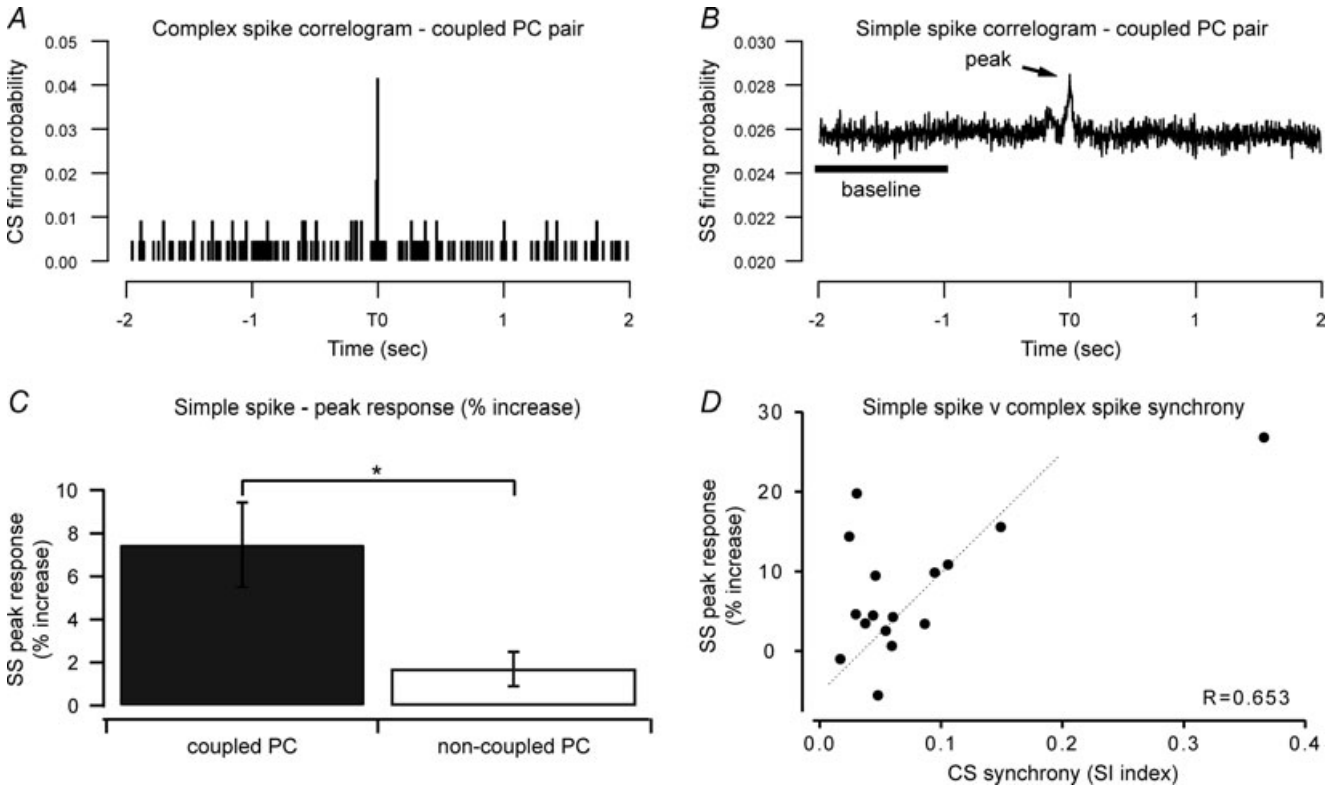

Figure 2. Synchrony in spontaneous complex spike activity
A, cross-correlogram of spontaneous complex spike activity from one coupled PC pair. A peak in the cross-correlogram at time zero indicates synchrony in the complex spike activity of these two cells (synchrony index, SI = 0.095). *B*, cross-correlogram of spontaneous simple spike activity from the same PC pair as shown in *A*. For this coupled PC pair there was a 9.9% increase in the correlogram peak (at time zero) above baseline level. *C*, mean (± S.E.M.) percentage change in peak probability of spontaneous simple spike activity for coupled and non-coupled pairs. *$P < 0.005$. *D*, individual data points of the peak responses from the simple spike cross-correlograms (% increase over baseline) plotted against complex spike synchrony index for coupled PC pairs only. There was a significant correlation between the level of simple spike and complex spike synchrony.

periods of time. There was a statistically significant peak in the cross-correlograms in a similar proportion of the coupled PC pairs (12/17, 70%).

By contrast, from a total of 15 non-coupled PCs recorded over a similar time period (one additional non-coupled PC pair was excluded because no simple spike activity was recorded in one of the cells), only 1/15 (7%) exhibited a statistically significant peak in their spontaneous simple spike cross-correlations. In the one case with a significant simple spike correlation, the complex spike firing rate in one of the paired cells was very low (0.05 Hz). It therefore remains a possibility that a weak temporal relationship in complex spike activity may have emerged for this particular pair of PCs if a larger sample size of complex spikes had been obtained.

Overall, the time zero peak in the simple spike cross-correlations for the 15 non-coupled PCs represented, relative to baseline levels of discharge, an average increase in the probability of synchronous firing of $1.7 \pm 0.8\%$. The increase in synchronous simple spike activity in coupled PCs as compared to non-coupled PCs was significantly different (Mann–Whitney test, $P < 0.005$, Fig. 2*C*).

To determine whether the magnitude of any simple spike correlation was a function of complex spike synchrony, linear regression analysis was performed (Fig. 2*D*). The percentage increase in the peak of the simple spike cross-correlogram was plotted against the complex spike synchrony index for each of the coupled PC pairs ($n = 16$). The results show a significant positive relationship ($r = 0.65$, ANOVA, $P < 0.01$), indicating that coupled PC pairs exhibiting higher complex spike synchrony also tend to exhibit a greater increase in the probability of synchrony in their simple spike firing.

To examine the possibility that PC pairs exhibiting correlated simple spike activity shared a common parallel fibre input, the location of such pairs in relation to the longitudinal axis of the folium was examined by determining the angle of orientation of the PC pair relative to the folium (see Fig. 1*C* and *D*). The dendritic arbour of individual PCs in fixed adult rat cerebellar tissue has been estimated to be about 220 μm in width (McKay & Turner, 2005). However, this value does not take into account shrinkage from the living state. We have therefore assumed a width of approximately 250 μm *in vivo*. Since each PC pair in the present study was separated by at least 500 μm (see Methods), the angle between them relative to the long axis of the folium should be less than 30 deg for the two PCs to have overlap between their dendritic trees and thereby share parallel fibre input. Six non-coupled PC pairs satisfied this criterion and none exhibited significant simple spike synchrony. Similarly, there were six coupled PC pairs with an angle of separation of less than 30 deg, and there was also no difference in the magnitude of simple spike synchrony between these pairs compared to the remaining coupled pairs. Moreover, coupled PC pairs were also observed in a parasagittal orientation and in some instances the paired cells were in adjacent lobules (Fig. 1*C* and *D*). Taken together these findings therefore suggest that 'on beam' parallel fibre activity is unlikely to fully explain the synchrony in simple spike activity we observed between coupled PCs.

Responses during peripheral stimulation

To examine the effects of peripheral afferent drive, the response of each PC to electrical stimulation of the ipsilateral forelimb and contralateral face was obtained. As a first step, PSTHs were constructed separately for complex spike and simple spike responses. Figure 3*A* demonstrates examples of PSTHs in response to peripheral stimulation for six individual PCs (Fig. 3*Aa–f*) recorded in three pairs (pairs 1–3). Pair 1 was coupled (SI = 0.054) with complex spike response latencies of 25 ms and peak firing probabilities of 0.41 (Fig. 3*Aa*) and 0.093 (Fig. 3*Ab*) to forelimb stimulation (978 stimuli presented). Pair 2 was weakly coupled (SI = 0.024) with a complex spike latency of 20 ms and peak response probability of 0.022 (Fig. 3*Ac*) to face stimulation (877 stimuli presented). The complex spike activity of the PC illustrated in Fig. 3*Ad* displayed only modest modulation to the peripheral stimulation. Pair 3 was non-coupled (SI = 0.01) with a complex spike response latency of 30 ms and peak response probability of 0.026 (Fig. 3*Ae*) and latency of 20 ms and peak response probability of 0.036 (Fig. 3*Af*) to face stimulation (501 stimuli presented).

The PSTH response profile for complex spike activity was used to help categorize the zonal origin of each PC. In the examples illustrated, the PCs in pair 1 were both located in the same zone (A2, ~500 μm apart), while for the PCs in pair 2 (~500 μm apart) and pair 3 (~700 μm apart), one PC was located in the A2 zone and the location of the other cell was unidentified (see Fig. 1*C* and *D* for location of PC pairs P1, P2 and P3). Overall, there was considerable variability in the patterns of response for both complex spike and simple spike activity, with increases and decreases in spike firing following stimulation. However, decreases were more reliably detected in the PSTHs constructed from simple spike activity, due to their much higher firing rates (thus higher bin counts). Rhythmic patterns of complex spike and simple spike modulation in response to the peripheral stimulation were only rarely observed and not studied further.

To provide an indication of the extent to which coupled as compared to non-coupled PCs exhibited similar (or dissimilar) patterns of response to peripheral stimulation, the PSTHs for complex spike and simple spike activity were assessed by comparing the spike counts in each time bin, and calculating a Pearson correlation coefficient (r).

For each PC pair, r values were calculated separately for comparison of PSTHs constructed for face stimulation and for forelimb stimulation. In Fig. 3*B* and *C* the highest Pearson correlation coefficient is plotted as a function of the corresponding complex spike synchrony index (SI) for each PC pair. Strongly coupled PC pairs (Fig. 3*B*, filled circles to the right of the plot) exhibited similar patterns of complex spike (Fig. 3*B*) *and* simple spike (Fig. 3*C*) response to peripheral stimulation as indicated by higher Pearson correlation coefficients. For example, in Fig. 3*A*, pair 1 had a complex spike SI = 0.054 and $r = 0.92$ for the PSTHs constructed from complex spike activity, and $r = 0.74$ for simple spike activity (Mann–Whitney rank sum test, $P < 0.0001$). Overall, coupled PC pairs as compared to non-coupled PCs displayed significantly higher Pearson coefficients (i.e. similar PSTH response profiles) for both complex spike ($n = 19$ coupled and $n = 16$ non-coupled PCs) and simple spike ($n = 17$ coupled and $n = 15$ non-coupled PCs) responses to peripheral stimulation (Fig. 3*D* and *E*, Mann–Whitney rank sum test, $P < 0.05$ in both comparisons). However, this relationship clearly was not without exceptions because: (i) some coupled PCs could exhibit rather different response profiles to the peripheral stimulation (Fig. 3*A*, pair 2, SI = 0.024 and $r = 0.15$ for complex spike activity and $r = 0.36$ for simple spike activity), and (ii) some non-coupled PCs displayed similar response profiles (Fig. 3*A*, pair 3, SI = 0.01 and $r = 0.58$ for complex spike activity (Mann–Whitney rank sum test, $P < 0.0001$) and $r = 0.24$ for simple spike activity, Mann–Whitney rank sum test, $P < 0.05$).

Complex spike synchrony during peripheral stimulation

Further analysis was undertaken to examine changes in complex spike synchrony as a result of activity evoked by peripheral stimulation. In this analysis shuffle-corrected cross-correlograms were generated to remove stimulus-locked effects (see Methods). A statistically significant correlation in complex spike activity during a post-stimulus response window of 0–500 ms occurred in 16/19 (84%) of the coupled PCs (i.e. the peak of the shuffle-corrected cross-correlogram exceeded 99% confidence limits). To evaluate whether coupled PCs showed any change over time in the degree of complex spike synchrony following peripheral

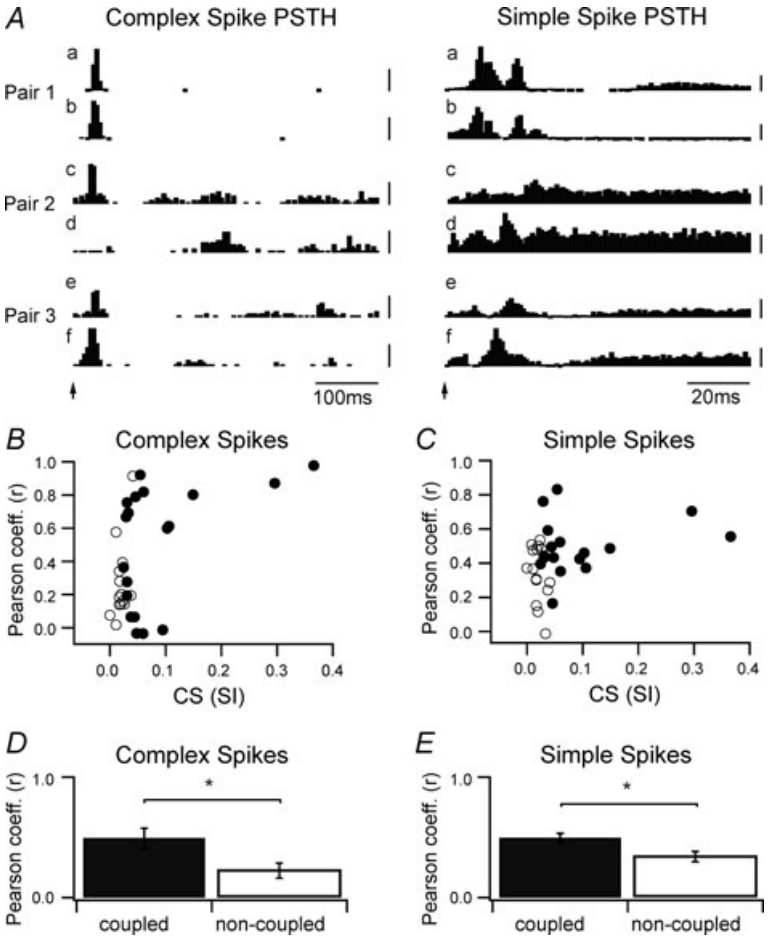

Figure 3. PC responses during peripheral stimulation
A, examples of PSTHs for complex spikes (5 ms bins) and simple spikes (1 ms bins) from six individual PCs in three pairs (pairs 1, 2 and 3; see Fig. 1*C* and *D* for pair location) in response to peripheral stimulation (arrow). Pair 1 (A2/A2 zone) was coupled (SI = 0.054) with complex spike response latencies of 25 ms to forelimb stimulation. PC pair 2 (A2/unidentified zone) was weakly coupled (SI = 0.024) with a complex spike latency of 20 ms to face stimulation (for the first PC). PC pair 3 (A2/unidentified zone) was non-coupled (SI = 0.01) with complex spike response latencies of 20–30 ms to face stimulation. Scale bars are firing probability: complex spikes (pair 1, –0.2 for top trace and 0.05 for second trace; pairs 2 and 3, –0.01); simple spikes (0.05). *B*, scatter plot of Pearson correlation coefficients (r) for complex spike PSTHs of all coupled (filled circles) and non-coupled (open circles) PC pairs plotted as a function of their complex spike synchrony index (SI). The PSTHs that yielded the highest Pearson coefficient was used in the analysis (i.e. highest value from face PSTH or forelimb PSTH). *C*, same as *B*, but scatter plot of Pearson correlation coefficients for simple spike PSTHs. *D*, mean (± S.E.M.) Pearson coefficient for complex spike PSTHs for all coupled and non-coupled PC pairs. *E*, same as *D*, but for simple spike PSTHs. $^*P < 0.05$.

stimulation, shuffle-corrected cross-correlograms were also constructed for two time periods after the face and forelimb stimulus (0–100 ms and 100–500 ms). Figure 4*A* shows the complex spike PSTHs for one coupled PC pair. In this example, the responses to peripheral stimulation are shown for a pair of PCs located in the A2 zone. Figure 4*B* shows the corresponding shuffle-corrected cross-correlogram for complex spikes occurring within the 0–100 ms post-stimulus time window (black bars), while Fig. 4*C* shows the shuffle-corrected cross-correlogram for complex spikes occurring within the 100–500 ms post-stimulus time window (black bars). These two shuffle-corrected cross-correlograms were compared to the cross-correlogram generated for spontaneous complex spike activity from the same pair of PCs (Fig. 4*B* and *C*, grey bars). By comparison to the amplitude of the cross-correlation time zero peak for spontaneous complex spike activity, there was a substantial increase (162% of spontaneous levels) in the probability of synchronous complex spike firing during the initial 0–100 ms post-stimulus period but in this example, there was a decrease (74% of spontaneous levels) during the 100–500 ms post-stimulus period.

Overall, the mean probability for complex spike synchrony in the 0–100 ms post-stimulus time period (0.1 ± 0.02) was significantly greater than both the mean probability of complex spike synchrony in the 100–500 ms post-stimulus time period (0.038 ± 0.015), and the probability of complex spike synchrony in the absence of a peripheral stimulus (spontaneous activity, 0.036 ± 0.01, ANOVA on ranks $P < 0.001$, $n = 19$). There was no significant difference in the probability of complex spike synchrony in the 100–500 ms post-stimulus time period as compared to the mean probability of synchronous activity in the absence of peripheral stimulation (ANOVA on ranks, $P = 0.3$). To examine differences in responses between face and forelimb stimulation, further *post hoc* analysis was carried out. This analysis indicated that synchrony data for both face and forelimb stimulation were significantly different to the spontaneous synchrony data in the 0–100 ms time period only (Fig. 4*D*, ANOVA on ranks, Student–Newman–Keuls method post test

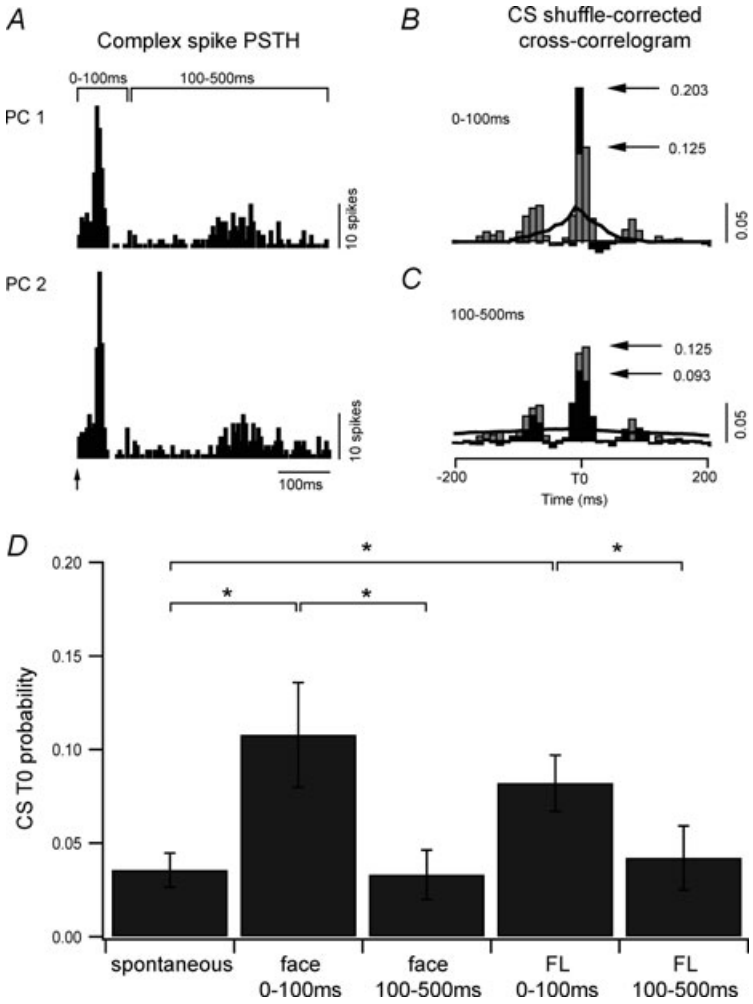

Figure 4. Complex spike synchrony during peripheral stimulation
A, PSTHs for two PCs in one coupled pair in response to electrical stimulation of the forelimb (arrow, 1175 stimuli). The post-stimulus response period was separated into two time windows, 0–100 ms and 100–500 ms and complex spikes occurring within these time periods were selected for the subsequent analysis. *B*, a shuffle-corrected cross-correlogram was generated from complex spike activity evoked during the 0–100 ms time window (black histogram) and compared to the cross-correlogram for spontaneous complex spikes (grey histogram, 10 ms bin width). Black line indicates 99% confidence level (scale bar 0.05 probability). *C*, same as *B*. but for the 100–500 ms time window. *D*, average complex spike cross-correlogram peak values for all coupled PC pairs ($n = 19$) for the two time windows (0–100 ms and 100–500 ms) in comparison to spontaneous activity. $^*P < 0.05$.

$P < 0.05$). For non-coupled PCs there was no significant difference between complex spike synchrony in all three datasets (0–100 ms, 100–500 ms and spontaneous data, ANOVA, $n = 16$, $P = 0.7$).

In 12/19 (63%) of the coupled PCs there was also an offset in the peak of the shuffle-corrected complex spike cross-correlograms during peripheral stimulation as compared to spontaneous activity. This was indicated by a difference in the timing of the peak (by greater than 2 ms) in the shuffle-corrected cross-correlograms, and became apparent when the cross-correlograms were constructed with 1–2 ms time bins, as opposed to the 10 ms bins used in the previous analysis. One PC pair exhibiting this phenomenon is shown in Fig. 5*A*. Since changes in synchronous complex spike activity were only evident in the initial 0–100 ms post-stimulus time window, the analysis of this phenomenon was confined to this time period. Figure 5*A* shows the shuffle-corrected complex spike cross-correlogram (black histogram) plotted together with the corresponding cross-correlogram for spontaneous complex spike activity for the same PC pair (grey histogram). Inspection of Fig. 5*A* shows a clear 10 ms difference in the timing of the peak during peripheral stimulation as compared to spontaneous activity (from 2 ms to −8 ms). In other words, while the timing of complex spikes in the two PCs during spontaneous activity was near synchronous (within 2 ms of each other), during peripheral stimulation the same two PCs display correlated complex spike activity with a time lag of 8 ms. Note that this difference in temporal coupling is not due to any independent but stimulus-locked differences in response of the two cells to peripheral stimulation: the shuffle-corrected cross-correlation analysis removes such effects from the correlogram.

Examination of the PSTHs for the PC pair shown in Fig. 5*A* also reveals a 10 ms difference in the response onset latency of the two PCs (Fig. 5*B*). The 'lead' PC in the cross-correlogram is the PC with the shorter latency to forelimb stimulation (PC1 in the example illustrated in Fig. 5*A*). This relationship was consistent for both face and forelimb stimulation with the lead PC always responding with the shorter latency. The pooled data indicate a strong positive correlation between the difference in response onset latency of each PC and the shift in the peak of the shuffle-corrected cross-correlogram for both face and forelimb stimulation (Fig. 5*C*, $n = 23$, Pearson coefficient $r = 0.95$, $P < 0.0001$). There was also a tendency for the PC with the shorter response latency to exhibit a greater probability of response to peripheral stimulation (as indicated in Fig. 5*B*), i.e. the lead PC typically exhibited greater responsiveness to the peripheral stimulus.

In some cases ($n = 5$) the lead PC in the shuffle-corrected cross-correlogram differed for face and forelimb stimulation, indicating that the lead PC can switch depending on the origin of the peripheral stimulus and related differences in onset latency. This switching phenomenon had a tendency to occur in coupled PC pairs with different zonal origins (3 of the 4 PC pairs were located in different zones). For example, when one PC was located in the A2 zone and the other PC was located in the C1 zone. Presumably this is because the two zones receive

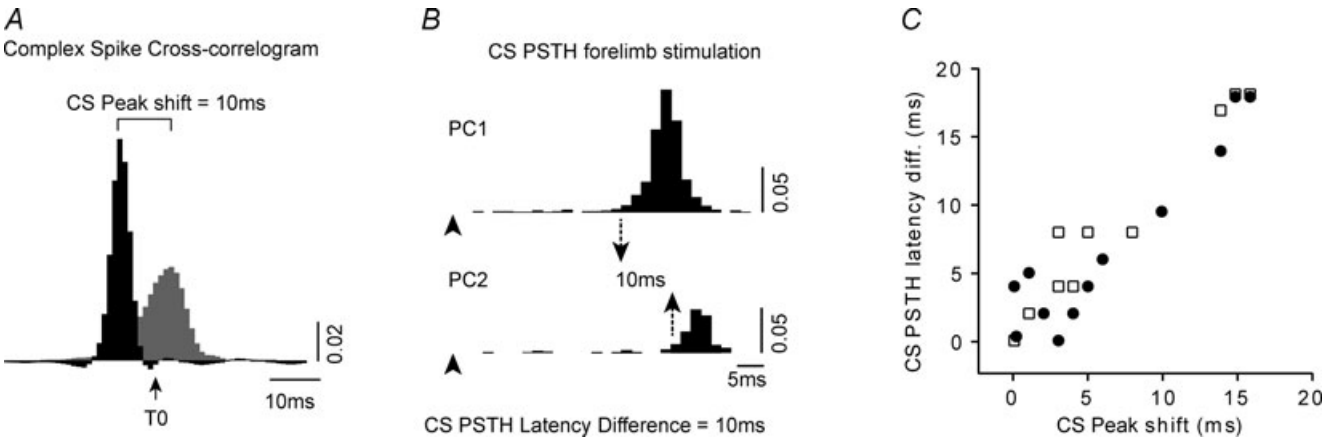

Figure 5. Temporal shift in complex spike cross-correlations during peripheral stimulation
A, two cross-correlograms, one of spontaneous complex spike (CS) activity (grey histogram) and the other, complex spike activity evoked during the 0–100 ms time window following forelimb stimulation (black histogram, 1 ms bin with 3 ms smoothing for both histograms, scale bar represents firing probability). In this example there was a 10 ms time shift in the peak of the two cross-correlograms. *B*, PSTHs for forelimb stimulation for the PC pair shown in *A*, demonstrating a 10 ms difference in the response onset latency. This difference was the same as the 10 ms shift in the peak of the shuffle-corrected cross correlogram. PC1 is the 'master' PC (i.e. the leading PC) in the cross-correlogram and has the shorter latency to forelimb stimulation. *C*, pooled data ($n = 23$) for the shift in the peak of the shuffle-corrected cross-correlogram (relative to spontaneous correlogram peak) plotted against the complex spikes PSTH latency differences for face (filled circles) and forelimb (open squares) stimulation.

their climbing fibre input from different subdivisions of the inferior olive, with corresponding differences in latency of climbing fibre signals conveyed from different body parts (cf. Atkins & Apps, 1997).

The shift in timing of the peak of the correlograms (time shift) highlights two novel features: firstly, a delayed temporal link exists between the two PCs that only becomes apparent during peripheral stimulation. Secondly, although the two PCs display synchronous complex spikes during spontaneous activity, this synchronous activity is absent in the presence of an incoming sensory afferent volley, i.e. the close synchrony present during spontaneous complex spike activity is no longer evident during peripheral stimulation (Fig. 5*A*).

The timing of any peaks for shuffle-corrected cross-correlograms using complex spikes in the 100–500 ms post-stimulus time period were similar to the timing of the peaks for the cross-correlograms constructed for spontaneous complex spike activity, suggesting that the time shift phenomenon was confined to the 100 ms time period immediately after the stimulus. Note also the difference in width of the two cross-correlograms in Fig. 5*A*. Typical of the data as a whole, the half-peak width of the cross-correlograms (using bin widths $\leq$5 ms with 3 ms Gaussian filter) from coupled PCs was greater during spontaneous activity than during evoked activity (one-way repeated measures ANOVA, $P < 0.002$, $n = 18$), i.e. the relative timing of complex spikes is temporally more dispersed for spontaneous than evoked activity.

Simple spike synchrony during stimulation

Shuffle-corrected cross-correlogram analysis was also used to establish whether there was any change in simple spike synchrony during peripheral stimulation. Figure 6*A* shows example PSTHs constructed for the simple spike activity of a coupled PC pair in which both cells responded primarily to the face stimulus (1 ms bins from the presentation of 1180 stimuli (arrow)). Figure 6*B* shows the shuffle-corrected cross-correlogram for the same PC pair (based on simple spike activity occurring in the 0–100 ms post-stimulus time period, since simple spike modulations occurred primarily during this time window). A statistically significant peak in the cross-correlogram is evident at time zero (dotted line indicates 99% confidence limit), indicating that the two PCs displayed synchronous simple spike activity following peripheral stimulation.

In 8 of the 17 coupled PCs (47%) a statistically significant increase in the peak in the shuffle-corrected cross-correlogram was also found for simple spike activity during the 0–100 ms response window (peak above 99% confidence limit). In contrast, only one of the 15 non-coupled PCs (7%) displayed a statistically significant increase in the probability of simple spike synchrony following peripheral stimulation (i.e. simple spikes within 1 ms of each other). The amplitude of the time zero peak was measured for each PC pair during spontaneous activity and during peripheral stimulation (for the 0–100 ms post-stimulus time window) and the

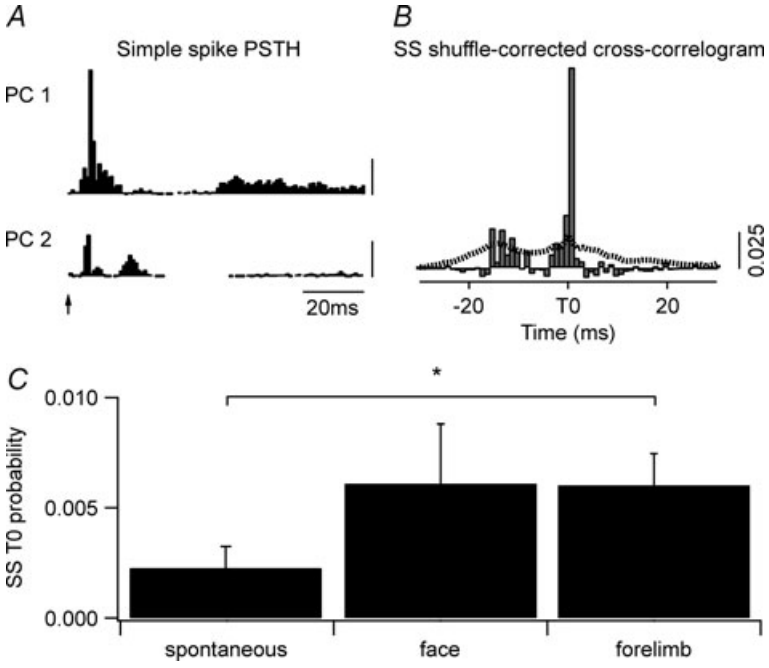

Figure 6. Simple spike synchrony during peripheral stimulation
A, simple spike (SS) PSTHs for two PCs from one coupled pair in response to face stimulation (1180 trials, stimulus at arrow). Simple spikes within the 0–100 ms time window were used for the subsequent cross-correlogram analysis (scale bar 0.025 probability). *B*, shuffle-corrected cross-correlogram (1 ms bins) of the data shown in *A*. Dotted line indicates 99% confidence level. *C*, mean size (± S.E.M.) of the time zero correlogram peaks for spontaneous simple spike activity and for simple spike activity evoked following face and forelimb stimulation for all coupled PC pairs ($n = 17$). *$P < 0.05$.

mean values (± S.E.M.) are shown in Fig. 6*C*. There was a statistically significant difference between time zero peaks measured following peripheral stimulation compared to spontaneous simple spike activity (Friedman repeated measures ANOVA, $P < 0.02$). However, *post hoc* analysis showed a significant difference for forelimb stimulation only (Dunn's method, $P < 0.05$). By contrast, for non-coupled PCs there was no significant difference in simple spike correlations following peripheral stimulation (Friedman repeated measures ANOVA, $P = 0.4$). Also, no time shift phenomenon was observed for simple spike activity.

Simple spike pauses

The frequency distribution of pause durations for individual PCs, i.e. the positive skewed tail of the associated interspike interval histogram) was not normal and typically could be fitted with an exponential function. In 20% of the sample of PCs there was also evidence of a bimodal distribution in their interspike interval histograms. This suggests that these cells tended to switch between firing simple spikes at either relatively high or low frequency. Up and down states have previously been reported in PCs (Loewenstein *et al.* 2005). However, the duration of pauses in the present study was much shorter than the prolonged periods (~3 s) of quiescence described by Loewenstein *et al.* (2005). For coupled PCs the median duration of the simple spike pauses was 129 ms (interquartile range 74–339 ms), while for non-coupled PCs the median pause duration was shorter (86 ms, interquartile range 66–133 ms). This difference was statistically significant (Mann–Whitney rank sum test, $P < 0.01$), suggesting that complex spike synchrony may play a role in determining pause duration (see below). The relationship between simple spike pauses and the occurrence of a complex spike was also examined. Cross-correlation analysis revealed a tendency for a pause in simple spike firing to occur at or before the onset of a complex spike and a cessation of a pause (i.e. a resumption of simple spike firing) to occur following a complex spike. There was also a tendency for an increase in spontaneous simple spike firing in the 30–100 ms time period immediately following a complex spike.

For coupled PCs there was also a significant increase in the probability that pauses in their simple spikes occurred synchronously (i.e. a correlation between pause on *versus* on, Fig. 7*A* and *D*). In other words, a long-lasting cessation

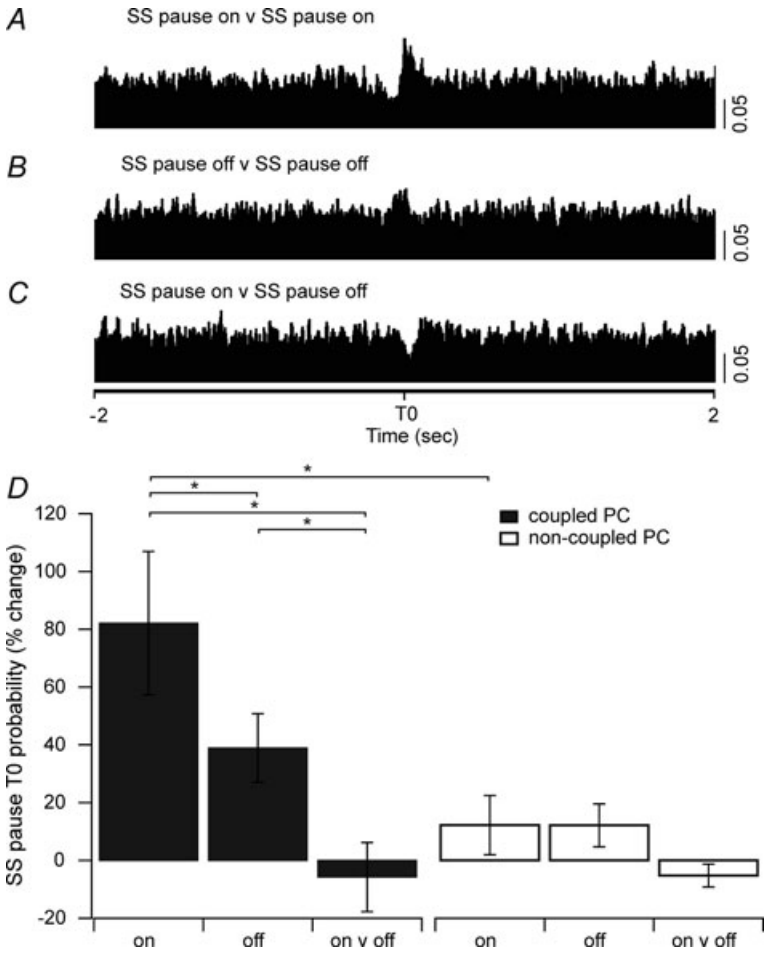

Figure 7. Cross-correlations in the timing of simple spike pauses
A, cross-correlation of the onset of a simple spike (SS) pause during spontaneous activity for one coupled PC pair (SS pause on *versus* SS pause on). *B*, the cessation of a pause (SS pause off *versus* SS pause off). *C*, the onset of a pause in one PC and the cessation of a pause in the other PC (SS pause on *versus* SS pause off). The onset and cessation of a simple spike pause was more likely to occur synchronously than the onset of a pause in one PC and the cessation of a pause in the other PC (5 ms bins, scale bar 0.05 probability for *A*–*C*). *D*, the means (± S.E.M.) of the change in simple spike pause T0 probability (%) shown for all coupled and non-coupled PC pairs for each of the three different pause conditions. *$P < 0.05$.

of simple spike activity in the two PCs was more likely to occur within 5 ms of each other than would be expected by chance with an 82.1 ± 24.8% ($n = 16$) increase in the probability at time zero (one-way repeated measures ANOVA, $n = 16$, $P < 0.001$). For cessation of pauses in coupled PCs, there was a significant increase in the probability that pauses in simple spikes would end within 5 ms of each other (pause off *versus* pause off, Fig. 7*B* and *D*), with an increase in probability of 38.9 ± 11.8% ($n = 16$) (one-way repeated measures ANOVA, $n = 16$, $P < 0.005$). *Post hoc* comparisons using the Holm–Sidak method indicated a significant difference in the time zero probability of 'pause on' compared to 'pause off' ($n = 16$, $P < 0.005$) indicating that there was a stronger temporal link in the onset of simple spike pauses compared to pause cessation in coupled PCs. The relationship between the onset of a pause in one cell and cessation of a pause in the other cell revealed a tendency for an average decrease: –5.7 ± 11.9% ($n = 16$) in the probability of a 'pause on' and a 'pause off' occurring within 5 ms of each other (Fig. 7*C* and *D*). That is, it was less likely that the cessation of simple spike activity in one cell was associated with the resumption of simple spike firing in the other. However, this effect was not statistically significant (one way repeated measures ANOVA, $n = 16$, $P = 0.26$).

The same pause analysis was also carried out on the simple spike firing patterns of non-coupled PCs (Fig. 7*D*). Although on average there was a 12.2 ± 10.3% increase in the probability that pause onset would start within 5 ms of each other (pause on *versus* on) this difference was not statistically significant (one-way repeated measures ANOVA, $n = 15$, $P = 0.3$). Similarly, there was a 12.1 ± 7.4% increase in likelihood that simple spike pauses in the two PCs would end within 5 ms of each other (pause off *versus* off) but again this difference was not statically significant (one-way repeated measures ANOVA, $n = 15$, $P = 0.3$). Finally, there was also a tendency for a decrease in the probability of a 'pause on' in one cell and a 'pause off' in the other cell occurring within 5 ms of each other, with an average of −5.2 ± 4.0%, but this was not significantly different from the baseline level (one-way repeated measures ANOVA, $n = 15$, $P = 0.3$).

Overall, coupled PCs were significantly more likely to exhibit correlations in the timing of simple spike pauses (both onset and offset) than non-coupled PCs. However, such an effect may be due to complex spike synchrony resulting in a temporal correlation in complex spike-induced cessation in simple spike activity. To test this possibility, all of the pauses in simple spike activity that occurred within 50 ms immediately after a complex spike were removed from the cross-correlation analysis. This had no appreciable effect on the results, suggesting that the correlation in simple spike pauses was independent of any temporal link in complex spike activity. However, since complex spike synchrony occurs not only in the pair of PCs recorded but also in other local PCs (see e.g. Lou & Bloedel, 1992; Welsh *et al.* 1995), this analysis does not rule out the possibility that complex spike activity in nearby PCs can modify simple spike pause activity. Finally, it is also of interest to consider the contribution of pauses to simple spike synchrony. By definition pauses represent only a small fraction (5%) of the simple spike inter-spike intervals (see Methods). Therefore removal of this small fraction from the spike train will *a priori* affect the correlation of the remaining bulk (95%) of the spike train by a small amount. For example, the PC pair that exhibited the greatest correlation in simple spike activity had a probability of firing for the time zero peak of $P = 0.0024$, compared to $P = 0.0023$ when all pauses were removed from the cross-correlation analysis. This represents ∼4% decrease in probability. In other words, pauses (as might be expected), make only a very minor contribution to simple spike synchrony.

Discussion

In the present study we report results for 35 simultaneously recorded pairs of PCs located mainly within the A2 or C1 zones in medial crus II and the paramedian lobule. Key findings were as follows. (1) Pairs of PCs with synchronous complex spike activity (coupled PCs) were more likely to also display synchrony in their simple spike activity (both spikes and pauses) than pairs of cells which lacked synchronous complex spike activity (non-coupled PCs). (2) Coupled PCs tended to exhibit similar patterns of complex spike and simple spike modulation to peripheral stimulation more than non-coupled PCs. (3) Coupled PCs also tended to increase their complex spike synchrony during peripheral stimulation but this effect was confined to the 100 ms post-stimulus time period. (4) Similar increases in simple spike synchrony were also observed in a 100 ms time window following peripheral stimulation. (5) For coupled PCs, the temporal relationship between their complex spike activity could be altered by peripheral stimulation and the shift in temporal correlation (including reversal of the timing relationship) depended on the source of that sensory stimulation. By contrast, no such shift could be found for the simple spike activity of coupled PCs.

Thus, PCs can be synchronously activated by both climbing fibre and mossy fibre inputs, and two independent mechanisms would appear to be in operation: one evident during spontaneous activity, the other when activity is influenced by sensory input.

Methodological considerations

Several factors may have influenced our findings. First, although ketamine anaesthesia is likely to be responsible

for the low average firing rates for complex spikes (0.53 Hz) and simple spikes (30.4 Hz, Bengtsson & Jorntell, 2007), such values are similar to those reported by others using different anaesthetics in rats (e.g. Cerminara & Rawson, 2004; Ros *et al.* 2009). Importantly, however, the effects of ketamine anaesthesia are unlikely to alter complex spike synchrony, as previous studies have shown that complex spike synchrony is similar in awake and ketamine-anaesthetized rats (Welsh *et al.* 1995; Lang *et al.* 1999; Schwarz & Welsh, 2001). Also, in the present study, both complex spike and simple spike synchrony and the related timing phenomena were not ubiquitous, which would suggest a non-specific anaesthetic effect. Instead, they were confined mainly to PC pairs located within the same cortical zone.

Complex spike synchrony

Synchrony in complex spike activity is thought to be due to one (or a weighted combination) of three mechanisms: climbing fibre branching (Armstrong *et al.* 1973*a*,*b*,*c*; Sugihara *et al.* 1995); electrotonic coupling between olive cells (e.g. Llinás *et al.* 1974); and/or synchronous afferent input driving activity in common groups of olive cells. PC pairs with a fixed (1:1) cross-correlation in their complex spike activity were not observed in the present study, suggesting that branching of an individual olivocerebellar axon to provide a climbing fibre to both PCs recorded as a pair was not responsible for the synchrony. This is unsurprising, given that the probability of two PCs sharing the same olivocerebellar axon is low (Llinás & Sasaki, 1989). Moreover, since correlations in timing of simple spike pauses were also present when complex spike activity in individual PCs was excluded from the analysis it also seems safe to conclude that such effects were not dependent on the direct influence of climbing fibre input on the PCs we recorded. Rather, any influence is likely to be a network effect (for further discussion see Schwarz & Welsh, 2001). This is further supported by the observation that the changes in synchrony (over about 100 ms) far outlasted the duration of the stimulus (0.1 ms), and by the finding that substantial time shifts in synchrony could occur between spontaneous and evoked activity.

The most thoroughly studied cerebellar network phenomenon is that of electrotonic coupling between olive cells, resulting in parasagittally aligned PCs firing complex spikes in synchrony (e.g. Llinás & Sasaki, 1989; Sasaki *et al.* 1989; Sugihara *et al.* 1993; Ozden *et al.* 2009). Such behaviour is thought to arise because neighbouring olive cells are electrically linked by dendrodendritic gap junctions (e.g. Llinás *et al.* 1974; Sotelo *et al.* 1974; Llinás & Sasaki, 1989; Sasaki *et al.* 1989; Welsh *et al.* 1995; De Zeeuw *et al.* 1996; Lang *et al.* 1996; Marshall *et al.* 2007), and also because of the intrinsic biophysical properties of olive cells (Llinás & Yarom, 1981*a*,*b*). Synchronous complex spike activity can also occur in the absence of afferent drive (Lang, 2001, 2003), emphasizing the importance of intrinsic olive networks in producing correlated activity. Previous studies have also emphasized the importance of oscillatory olivary activity in gating sensory inputs to the cortex (Llinás & Sasaki, 1989), and in modulating simple spike rhythmic activity (Schwarz & Welsh, 2001). However, rhythmic activity was only rarely observed in the present study.

Our results suggest that mechanisms besides electrotonic coupling may also be involved in generating complex spike synchrony. In particular, PC pairs can show relatively broad peaks in their complex spike cross-correlograms ($>$20 ms), as reported here, and previously (Bell & Kawasaki, 1972; Wylie *et al.* 1995). By contrast, axon-reflex experiments have estimated that olive cells targeting the same parasagittal strip of cortex are linked electrotonically with a temporal dispersion of 1–2 ms (Llinás & Sasaki, 1989), suggesting that cross-correlations would have much sharper peaks if electrotonic coupling was the principal mechanism responsible for synchrony. More recently, Marshall & Lang (2009) have also shown that the level of complex spike synchrony can be regulated by simple spike activity through the cortico-nucleo-olivary loop. Whether this includes synchronous simple spike activity from PCs in the same zone, as seen in the present study remains to be determined. An additional consideration is the highly dynamic patterns of response we observed to peripheral stimulation, including substantial time shifts in complex spike synchrony and switches in lead PC (see also below). These phenomena would seem difficult to explain purely on the basis of electrotonic coupling between olive cells. However, it remains a possibility that the peripheral stimulus generates a travelling wave in the olive that starts from the lead cell and propagates to neighbouring olivary regions to evoke activity with an appropriate delay (cf. Devor & Yarom, 2002).

Simple spike synchrony

PCs that showed coupled complex spike synchrony also displayed simple spike synchrony. Coupled PCs showed no obvious spatial relationship in relation to simple spike synchrony although synchrony occurred most frequently in PCs located in the same rostro-caudally oriented climbing fibre zone. In some instances, coupling spanned across two lobules indicating that simple spike synchrony cannot be due solely to on-beam parallel fibre synchrony (cf. Heck *et al.* 2007). Rather, one or more of the following factors may be involved: common sources of mossy fibre afferents (Voogd *et al.* 2003; Pijpers *et al.* 2006); climbing fibre activation of cerebellar cortical interneurones (Lemkey-Johnston & Larramendi, 1968; Schulman & Bloom, 1981; Sugihara *et al.* 2001; Xu &

Edgley, 2008); and/or inhibitory collaterals of PC axons acting on cortical interneurones (Hamori & Szentagothai, 1968; McCrea *et al.* 1976; De Zeeuw *et al.* 1994). In addition to these cortical network possibilities, complex spike synchrony converging downstream on non-GABAergic cerebellar nuclear targets may also lead to an increase in excitatory input to several precerebellar mossy fibre targets that could, in turn, generate synchronous simple spike activity through common afferent drive (reviewed by Ruigrok & Cella, 1995). Further experiments are required to determine which of these factors contribute to the observed synchrony in simple spike activity.

Complex spike and simple spike temporal relations

Few studies have previously recorded multiple PCs simultaneously with sufficient signal-to-noise resolution to reliably discriminate both complex spike and simple spike activity from the same cells. De Zeeuw *et al.* (1997) reported in awake rabbits that a sample of 10 PC pairs recorded in the flocculus had levels of synchrony between complex spike and simple spike activity that were positively correlated, with the highest correlations occurring between PC pairs located within the same zone. A similar relationship was also noted (but not quantified) for a small sample of PC pairs in the pentobarbitone-anaesthetized cat (Bell & Grimm, 1969) and guinea pig (Bell & Kawasaki, 1972). The present findings, together with these previous studies, therefore suggest that synchronization of complex spike and simple spike activity can be recorded in a range of species; occurs in the anaesthetized and unanaesthetized animal; and is present in a number of different cerebellar zones (vermal, paravermal and floccular). Thus, temporal correlations in both complex spike and simple spike activity for PCs located within the same zone would seem to be a general feature of cerebellar information processing.

Effects of evoked activity on synchrony

The present results are also consistent with previous studies which have shown that afferent drive can increase complex spike synchrony (Llinás & Sasaki, 1989; Lou & Bloedel, 1992; Welsh *et al.* 1995; Wylie *et al.* 1995; Lang, 2002; Schultz *et al.* 2009). However, previous studies have not investigated the effects of sensory afferent stimulation on both complex spike and simple spike synchrony. The only previous study used electrical stimulation of the tongue area of the motor cortex in ketamine-anaesthetized rats to generate 'long lasting and highly dynamic' patterns of modulation of complex spike and simple spike synchrony and rhythmicity (Schwarz & Welsh, 2001). In marked contrast to our findings, they found that the degree of complex spike synchrony was ***reduced*** during the initial 150 ms time period post stimulus, but increased during the subsequent 150–275 ms. Their results also differ significantly from ours in that a large percentage (33/42, 79%) of their sample of PCs fired simple spikes rhythmically (at a rate of about 75 Hz). The reason for these differences remains to be determined but presumably relates to the source of the afferent stimulation (motor cortex *versus* periphery) and/or the site of cerebellar recording (medial *versus* lateral aspects of crus II). For the latter, it may be relevant to note that the medial and lateral hemisphere may be functionally distinct (Sugihara, 2006).

Functional implications and concluding comments

PCs located within each cortical zone project to different regions of the cerebellar and vestibular nuclei to produce monosynaptic inhibition of their target neurones. Anatomically, about 900 PCs converge onto each cerebellar nuclear neurone (Palkovits *et al.* 1977). In turn, the efferent neurones from these nuclei powerfully excite motor cell groups belonging to medial and lateral descending motor paths. PCs therefore have a rather direct influence on activity in descending motor pathways (for review see Armstrong, 1986).

Experiments using whole-cell patch-clamping of cerebellar nuclear cells using dynamic clamping techniques to investigate excitatory and inhibitory inputs have found that correlated activity in populations of PCs is well suited to the dynamic control of cerebellar nuclear activity (Gauck & Jaeger, 2000, 2003). The present study provides evidence *in vivo* that PCs located in the same cerebellar zone can be synchronously activated by both climbing fibre and mossy fibre inputs. Two mechanisms appear to be in operation to regulate PC synchrony: one is evident during spontaneous activity, the other during sensory afferent drive. Whilst previous studies have emphasized electrotonic coupling as underlying complex spike synchrony, the present results indicate that afferent drive reveals an additional mechanism underlying complex spike ***and*** simple spike synchrony. The relative importance of these two mechanisms remains to be defined. Nevertheless, the synchronous activity is likely to have a significant effect on cortical output to the corresponding cerebellar nuclear territory and thus have a profound influence on cerebellar contributions to motor control. In particular, the temporal relationships in simple spike pauses occurring primarily in coupled PC pairs provides a mechanism through which zonally organized PCs could modulate activity in their target cerebellar nuclear cells. Evidence suggests that the duration of pauses in simple spike firing represents an important coding mechanism for learned patterns of parallel fibre activation (Steuber *et al.* 2007). The synchronized occurrence of simple spike pauses in ensembles of PCs that converge onto the same population of cerebellar nuclear neurones could

elicit a rebound depolarization through disinhibition (Aizenman & Linden, 1999), and thereby trigger bursts of activity in a specific group of cerebellar output neurones. Consistent with this possibility is the finding that the effectiveness of a PC simple spike pause to elicit rebound nuclear burst activity has been shown to depend on the synchrony of the disinhibition produced by the pause (Shin & De Schutter, 2006; Steuber *et al.* 2007). Rebound bursts of synchronous activity in cerebellar nuclear cells may therefore represent an important timing signal to drive coordinated patterns of muscle contraction during movement.

References

Aizenman CD & Linden DJ (1999). Regulation of the rebound depolarization and spontaneous firing patterns of deep nuclear neurons in slices of rat cerebellum. *J Neurophysiol* **82**, 1697–1709.

Apps R & Garwicz M (2005). Anatomical and physiological foundations of cerebellar information processing. *Nat Rev Neurosci* **6**, 297–311.

Apps R & Hawkes R (2009). Cerebellar cortical organization: a one-map hypothesis. *Nat Rev Neurosci* **10**, 670–681.

Armstrong DM (1986). Supraspinal contributions to the initiation and control of locomotion in the cat. *Prog Neurobiol* **26**, 273–361.

Armstrong DM, Harvey RJ & Schild RF (1973*a*). Cerebello-cerebellar responses mediated via climbing fibres. *Exp Brain Res* **18**, 19–39.

Armstrong DM, Harvey RJ & Schild RF (1973*b*). The spatial organisation of climbing fibre branching in the cat cerebellum. *Exp Brain Res* **18**, 40–58.

Armstrong DM, Harvey RJ & Schild RF (1973*c*). Spino-olivocerebellar pathways to the posterior lobe of the cat cerebellum. *Exp Brain Res* **18**, 1–18.

Armstrong DM & Rawson JA (1979). Activity patterns of cerebellar cortical neurones and climbing fibre afferents in the awake cat. *J Physiol* **289**, 425–448.

Atkins MJ & Apps R (1997). Somatotopical organisation within the climbing fibre projection to the paramedian lobule and copula pyramidis of the rat cerebellum. *J Comp Neurol* **389**, 249–263.

Bell CC & Grimm RJ (1969). Discharge properties of Purkinje cells recorded on single and double microelectrodes. *J Neurophysiol* **32**, 1044–1055.

Bell CC & Kawasaki T (1972). Relations among climbing fiber responses of nearby Purkinje cells. *J Neurophysiol* **35**, 155–169.

Bengtsson F & Jorntell H (2007). Ketamine and xylazine depress sensory-evoked parallel fiber and climbing fiber responses. *J Neurophysiol* **98**, 1697–1705.

Cerminara NL, Apps R & Marple-Horvat DE (2009). An internal model of a moving visual target in the lateral cerebellum. *J Physiol* **587**, 429–442.

Cerminara NL & Rawson JA (2004). Evidence that climbing fibers control an intrinsic spike generator in cerebellar Purkinje cells. *J Neurosci* **24**, 4510–4517.

Devor A & Yarom Y (2002). Generation and propagation of subthreshold waves in a network of inferior olivary neurons. *J Neurophysiol* **87**(6), 3059–69.

De Zeeuw CI, Koekkoek SK, Wylie DR & Simpson JI (1997). Association between dendritic lamellar bodies and complex spike synchrony in the olivocerebellar system. *J Neurophysiol* **77**, 1747–1758.

De Zeeuw CI, Lang EJ, Sugihara I, Ruigrok TJ, Eisenman LM, Mugnaini E & Llinás R (1996). Morphological correlates of bilateral synchrony in the rat cerebellar cortex. *J Neurosci* **16**, 3412–3426.

De Zeeuw CI, Wylie DR, DiGiorgi PL & Simpson JI (1994). Projections of individual Purkinje cells of identified zones in the flocculus to the vestibular and cerebellar nuclei in the rabbit. *J Comp Neurol* **349**, 428–447.

Drummond, GB (2009). Reporting ethical matters in *The Journal of Physiology*: standards and advice. *J Physiol* **587**, 713–719.

Eccles JC, Llinás R & Sasaki K (1966). The excitatory synaptic action of climbing fibres on the Purkinje cells of the cerebellum. *J Physiol* **182**, 268–296.

Gauck V & Jaeger D (2000). The control of rate and timing of spikes in the deep cerebellar nuclei by inhibition. *J Neurosci* **20**, 3006–3016.

Gauck V & Jaeger D (2003). The contribution of NMDA and AMPA conductances to the control of spiking in neurons of the deep cerebellar nuclei. *J Neurosci* **23**, 8109–8118.

Gerstein GL & Perkel DH (1972). Mutual temporal relationships among neuronal spike trains. Statistical techniques for display and analysis. *Biophys J* **12**, 453–473.

Hamori J & Szentagothai J (1968). Identification of synapses formed in the cerebellar cortex by Purkinje axon collaterals: an electron microscope study. *Exp Brain Res* **5**, 118–128.

Häusser M & Clark BA (1997). Tonic synaptic inhibition modulates neuronal output pattern and spatiotemporal synaptic integration. *Neuron* **19**, 665–678.

Heck DH, Thach WT & Keating JG (2007). On-beam synchrony in the cerebellum as the mechanism for the timing and coordination of movement. *Proc Nat Acad Sci U S A* **104**, 7658–7663.

Hounsgaard J & Midtgaard J (1988). Intrinsic determinants of firing pattern in Purkinje cells of the turtle cerebellum *in vitro*. *J Physiol* **402**, 731–749.

Lang EJ (2001). Organization of olivocerebellar activity in the absence of excitatory glutamatergic input. *J Neurosci* **21**, 1663–1675.

Lang EJ (2002). GABAergic and glutamatergic modulation of spontaneous and motor-cortex-evoked complex spike activity. *J Neurophysiol* **87**, 1993–2008.

Lang EJ (2003). Excitatory afferent modulation of complex spike synchrony. *Cerebellum* **2**, 165–170.

Lang EJ, Sugihara I & Llinás R (1996). GABAergic modulation of complex spike activity by the cerebellar nucleoolivary pathway in rat. *J Neurophysiol* **76**, 255–275.

Lang EJ, Sugihara I, Welsh JP & Llinás R (1999). Patterns of spontaneous Purkinje cell complex spike activity in the awake rat. *J Neurosci* **19**, 2728–2739.

Lemkey-Johnston N & Larramendi LM (1968). Types and distribution of synapses upon basket and stellate cells of the mouse cerebellum: an electron microscopic study. *J Comp Neurol* **134**, 73–112.

Llinás R, Baker R & Sotelo C (1974). Electrotonic coupling between neurons in cat inferior olive. *J Neurophysiol* **37**, 560–571.

Llinás R & Sasaki K (1989). the functional organization of the olivo-cerebellar system as examined by multiple Purkinje cell recordings. *Eur J Neurosci* **1**, 587–602.

Llinás R & Sugimori M (1980). Electrophysiological properties of *in vitro* Purkinje cell somata in mammalian cerebellar slices. *J Physiol* **305**, 171–195.

Llinás R & Yarom Y (1981*a*). Electrophysiology of mammalian inferior olivary neurones *in vitro*. Different types of voltage-dependent ionic conductances. *J Physiol* **315**, 549–567.

Llinás R & Yarom Y (1981*b*). Properties and distribution of ionic conductances generating electroresponsiveness of mammalian inferior olivary neurones *in vitro*. *J Physiol* **315**, 569–584.

Loewenstein Y, Mahon S, Chadderton P, Kitamura K, Sompolinsky H, Yarom Y & Häusser M (2005). Bistability of cerebellar Purkinje cells modulated by sensory stimulation. *Nat Neurosci* **8**, 202–211.

Lou JS & Bloedel JR (1992). Responses of sagittally aligned Purkinje cells during perturbed locomotion: synchronous activation of climbing fiber inputs. *J Neurophysiol* **68**, 570–580.

McCrea RA, Bishop GA & Kitai ST (1976). Intracellular staining of Purkinje cells and their axons with horseradish peroxidase. *Brain Res* **118**, 132–136.

McKay BE & Turner RW (2005). Physiological and morphological development of the rat cerebellar Purkinje cell. *J Physiol* **567**, 829–850.

Marshall SP & Lang EJ (2009). Local changes in the excitability of the cerebellar cortex produce spatially restricted changes in complex spike synchrony. *J Neurosci* **29**, 14352–14362.

Marshall SP, Van Der Giessen RS, De Zeeuw CI & Lang EJ (2007). Altered olivocerebellar activity patterns in the connexin36 knockout mouse. *Cerebellum* **6**, 287–299.

Ozden I, Sullivan MR, Lee HM & Wang SS (2009) Reliable coding emerges from coactivation of climbing fibers in microbands of cerebellar Purkinje neurons. *J Neurosci* **29**, 10463–10473.

Palkovits M, Mezey E, Hamori J & Szentagothai J (1977). Quantitative histological analysis of the cerebellar nuclei in the cat. I. Numerical data on cells and on synapses. *Exp Brain Res* **28**, 189–209.

Pardoe J & Apps R (2002). Structure–function relations of two somatotopically corresponding regions of the rat cerebellar cortex: olivo-cortico-nuclear connections. *Cerebellum* **1**, 165–184.

Pijpers A, Apps R, Pardoe J, Voogd J & Ruigrok TJ (2006). Precise spatial relationships between mossy fibers and climbing fibers in rat cerebellar cortical zones. *J Neurosci* **26**, 12067–12080.

Ros H, Sachdev RN, Yu Y, Sestan N & McCormick DA (2009). Neocortical networks entrain neuronal circuits in cerebellar cortex. *J Neurosci* **29**, 10309–10320.

Ruigrok TJ & Cella F (1995). Precerebellar nuclei and red nucleus. In *The Rat Nervous System*, ed. Paxinos G, pp. 277–308. Academic Press, Sydney.

Sasaki K, Bower JM & Llinás R (1989). Multiple Purkinje cell recording in rodent cerebellar cortex. *Eur J Neurosci* **1**, 572–586.

Schulman JA & Bloom FE (1981). Golgi cells of the cerebellum are inhibited by inferior olive activity. *Brain Res* **210**, 350–355.

Schultz SR, Kitamura K, Post-Uiterweer A, Krupic J & Häusser M (2009). Spatial pattern coding of sensory information by climbing fiber-evoked calcium signals in networks of neighboring cerebellar Purkinje cells. *J Neurosci* **29**, 8005–8015.

Schwarz C & Welsh JP (2001). Dynamic modulation of mossy fiber system throughput by inferior olive synchrony: a multielectrode study of cerebellar cortex activated by motor cortex. *J Neurophysiol* **86**, 2489–2504.

Shin SL & De Schutter E (2006). Dynamic synchronization of Purkinje cell simple spikes. *J Neurophysiol* **96**, 3485–3491.

Sotelo C, Llinás R & Baker R (1974). Structural study of inferior olivary nucleus of the cat: morphological correlates of electrotonic coupling. *J Neurophysiol* **37**, 541–559.

Steuber V, Mittmann W, Hoebeek FE, Silver RA, De Zeeuw CI, Häusser M & De Schutter E (2007). Cerebellar LTD and pattern recognition by Purkinje cells. *Neuron* **54**, 121–136.

Sugihara I (2006). Organization and remodeling of the olivocerebellar climbing fiber projection. *Cerebellum* **5**, 15–22.

Sugihara I, Lang EJ & Llinás R (1993). Uniform olivocerebellar conduction time underlies Purkinje cell complex spike synchronicity in the rat cerebellum. *J Physiol* **470**, 243–271.

Sugihara I, Lang EJ & Llinás R (1995). Serotonin modulation of inferior olivary oscillations and synchronicity: a multiple-electrode study in the rat cerebellum. *Eur J Neurosci* **7**, 521–534.

Sugihara I, Wu HS & Shinoda Y (2001). The entire trajectories of single olivocerebellar axons in the cerebellar cortex and their contribution to cerebellar compartmentalization. *J Neurosci* **21**, 7715–7723.

Thach WT (1968). Discharge of Purkinje and cerebellar nuclear neurons during rapidly alternating arm movements in the monkey. *J Neurophysiol* **31**, 785–797.

Thach WT (1967). Somatosensory receptive fields of single units in cat cerebellar cortex. *J Neurophysiol* **30**, 675–696.

Voogd J & Glickstein M (1998). The anatomy of the cerebellum. *Trends Neurosci* **21**, 370–375.

Voogd J, Pardoe J, Ruigrok TJ & Apps R (2003). The distribution of climbing and mossy fiber collateral branches from the copula pyramidis and the paramedian lobule: congruence of climbing fiber cortical zones and the pattern of zebrin banding within the rat cerebellum. *J Neurosci* **23**, 4645–4656.

Welsh JP, Lang EJ, Sugihara I & Llinás R (1995). Dynamic organization of motor control within the olivocerebellar system. *Nature* **374**, 453–457.

Welsh JP & Llinás R (1997). Some organizing principles for the control of movement based on olivocerebellar physiology. *Prog Brain Res* **114**, 449–461.

Woodward DJ, Hoffer BJ & Altman J (1974). Physiological and pharmacological properties of Purkinje cells in rat cerebellum degranulated by postnatal x-irradiation. *J Neurobiol* **5**, 283–304.

Wylie DR, De Zeeuw CI & Simpson JI (1995). Temporal relations of the complex spike activity of Purkinje cell pairs in the vestibulocerebellum of rabbits. *J Neurosci* **15**, 2875–2887.

Xu W & Edgley SA (2008). Climbing fibre-dependent changes in Golgi cell responses to peripheral stimulation. *J Physiol* **586**, 4951–4959.

Author contributions

A.K.W., D.E.M.-H. and R.A. conceived and designed the experiments; A.K.W. carried out the experiments; A.K.W. and N.L.C. performed data analysis; A.K.W., D.E.M.-H. and R.A. drafted the paper; A.K.W., N.L.C., D.E.M.-H. and R.A. revised the paper. All authors approved the final version of the manuscript.

Acknowledgements

This work was supported by the Wellcome Trust.